

Tracking Control for a Two-Wheel Differentially Driven Nonholonomic Mobile Robot: Performance Comparison

Fadwa Al-Momani, Asma Al-Tamimi, Ahmad Al-Jarrah, Ayat Al-Jarrah, and Mohammad Salah
 Department of Mechatronics Engineering, Faculty of Engineering, The Hashemite University, Zarqa, Jordan
 Email: {fadwamomani, altamimi, jarrah, ayataljarrah, msalah}@hu.edu.jo

Abstract—This research study aims to investigate various trajectory tracking control techniques for two-wheel mobile robots. First, a discrete optimal control technique is formulated to track time-varying desired trajectories, and then the performance is compared with the performance of discrete PID and fuzzy controllers. To design the discrete optimal controller, a Riccati equation is solved from a developed discrete-time linear model for the two-wheel mobile robot dynamics. Multiple numerical simulations are introduced to investigate the effectiveness of the proposed controllers.

Index Terms—discrete optimal control, discrete PID, fuzzy control, two-wheel mobile robot

k_b	voltage coefficient of mobile robot wheels' motors
I_{ar}, I_{al}	right and left armature currents of mobile robot wheels' motors
V_r, V_l	control input voltages applied on the right and left mobile robot wheels' motors
τ_{Lr}, τ_{Ll}	load torques applied on the right and left mobile robot wheels motors due to the robot weight and wheels' friction with the ground
U^*	optimal control law
U	control law
V	linear velocity of mobile robot

NOMENCLATURE TABLE

Parameter	Description
x, y	x and y coordinates of mobile robot
\dot{x}, \dot{y}	x and y change rate of mobile robot
x_d, y_d	desired x, y
θ	angular position (orientation angle) of mobile robot
$\dot{\theta}$	angular velocity (orientation angle change rate) of mobile robot around its center
θ_d	desired θ
v_x, v_y	linear velocities of mobile robot in x and y directions
ω_r, ω_l	right and left angular velocities of mobile robot wheels
ω	angular velocity (orientation angle change rate) of mobile robot around its center
ω_d	desired ω
r	radius of mobile robot wheels
d	distance between the two wheels of mobile robot
J	inertial of mobile robot wheels' motors
B	viscous friction coefficient of mobile robot wheels' motors
R_a	armature resistance of mobile robot wheels' motors
L_a	armature inductance of mobile robot wheels' motors
k_m	torque coefficient of mobile robot wheels' motors

I. INTRODUCTION

The domain of mobile robot control has been the focus of active research for decades. A mobile robot is a machine that can combine artificial intelligence and physical devices that are capable of moving in the surrounding. It proved its necessity in industrial, military, health care, distribution of goods, and many other applications in other fields [1].

Controlling such systems requires understanding the model of the system which includes the kinematics and dynamics [2]. Since the system under study is a differential drive two-wheel mobile robot, it will be constrained to move in the lateral direction that is known as a nonholonomic system [3]. Moreover, since the main task is to control the movement of the two-wheel mobile robot to have a smooth trajectory tracking, this requires realizing the motion algorithms of the system, which is known as path planning. Those algorithms are used to describe the movement of mobile robots and to finally find an optimal path like “ant colony optimization algorithm” [4]. Other algorithms used laser tools to build 3D maps of large, cyclic environments in real-time [5]. Weighted line fitting algorithms are also used to build the map for mobile robots movement [6].

Furthermore, discrete methodologies have a wide range of applications; for instance, discrete controls are designed to control the two-wheel mobile robot movement [7]. A discrete artificial potential field algorithm is used for the path planning approach [8] and a fuzzy discrete has been

used to model the system [9]. On the other hand, Proportional-Integral-Derivative (PID) and fuzzy logic algorithms are the most common methods used to control mobile robots. In [10], a fuzzy logic controller was introduced to track the desired path utilizing distance and orientation errors. The authors of [11] introduced 153 fuzzy rules for tracking desired paths where these rules utilized the distant and the orientation errors within a real-time experiment and U-shaped hurdle environment. Optical navigation that is based on fuzzy logic and optimum flow approach was presented by the authors of [12] where its parameters were calculated by the Horn-Schunk algorithm. A PID controller was designed to drive a mobile robot in order to track a desired trajectory such as the one used in [13]. Responses of the robot in the square-shaped trajectory were obtained with a small error. Some controllers combined a fuzzy logic with a PID to get a fast-tracking with a minimal overshoot in comparison with the traditional PID or fuzzy logic controllers [14].

Moreover, adaptive fuzzy logic control for line tracking was presented in [15] where a new control scheme combined PD and fuzzy logic controllers. This control scheme showed a good steady-state tracking performance. The results showed an exceedingly small error and fast convergence towards the desired trajectory in a short period of time. A new behavior-based fuzzy method was presented in [16]. This method considered angular velocities of the wheels as outputs, and it introduced a limited number of intermediate variables to guarantee the uniformity of the fuzzy rule bases. Multiple-Input Multiple-Output (MIMO) fuzzy control for independent mobile robots addressed the design and implementation of control systems by [17]. MIMO fuzzy was applied to track different desired trajectories. Furthermore, a robust adaptive trajectory tracking controller was introduced in [18] to compensate for the effects of dynamic disturbance and improve the adaptive switching control to diminish the chattering phenomenon and optimize the convergence rate. However, the proposed controller was designed to be discrete in order to be less affected by noisy signals. In addition, it was designed to be optimum to optimize the performance in terms of error and effort.

A trajectory tracking controller was also designed and proposed for a two-wheeled mobile robot, named Kian-I, to facilitate accurate navigation in an immersive environment [19]. The error between the desired path and the followed trajectory was eliminated by utilizing the wheels' velocity. In [20], the authors presented an Automated Guided Vehicles (AGV) robot group focusing on the control part that drives the (AGV) to track certain paths. Ziegler-Nichols and empirical methods were utilized for tuning the PID controller. Finally, bio-inspired optimization algorithms, such as Particle Swarm Optimization (PSO), Artificial Bee Colony (ABC), and Firefly Algorithm (FA), along with a PID control were utilized to determine a collision-free path through fixed obstacles in the working environment [21]. The proposed

controller was applied to a two-wheeled mobile robot on a real platform and the results were satisfactory.

This paper¹ presents a trajectory tracking discrete optimal control design for two-wheel mobile robots that can handle the unknown disturbances associated with their motion. The preliminary version of this study, in [22], presented only the design of the optimal controller and showed the simulation performance results under a circular trajectory. However, the work in [22] has been extended, in this article, by testing the proposed discrete optimal controller with different trajectories and by comparing the performance with a discrete PID and fuzzy logic controllers to investigate the validity of the proposed controller.

The rest of the paper is organized as follows; Section II presents the mathematical modeling of the two-wheel mobile robot kinematics and dynamics, Section III explains the development of the proposed discrete optimal controller. Sections IV and V introduce a discrete PID controller and a fuzzy logic controller for the sake of comparison with the discrete optimal controller. Finally, Section VI demonstrates numerical simulations and Section VII presents the conclusions.

II. MATHEMATICAL MODELING

Mobile robot kinematic and dynamic models are well described in the literature for various structures and frameworks as shown in [23]. The proposed two-wheel mobile robot is depicted in Fig. 1. From the figure, it is clear that a differential drive is essential to maneuver the mobile robot and determine its motion trajectory. To understand how the right and left wheels' motion affect the behavior of the entire mobile robot, its kinematics and dynamics should be understood.

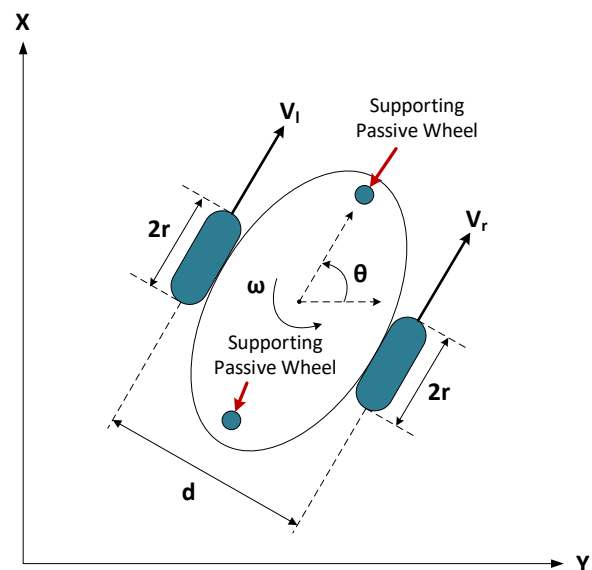


Figure 1. The proposed two-wheel mobile robot.

¹ A preliminary version of this work has appeared in [22].

A. Kinematics of Two-Wheel Mobile Robot

The kinematics of the proposed two-wheel mobile robot is well established in the literature. However, it can be presented in different ways. The continuous-time version of the kinematics can be described as follows

$$\begin{bmatrix} \dot{x} \\ \dot{y} \\ \dot{\theta} \end{bmatrix} = \begin{bmatrix} v_x \\ v_y \\ \omega \end{bmatrix} = \begin{bmatrix} \frac{r}{2} \cos \theta & \frac{r}{2} \cos \theta \\ \frac{r}{2} \sin \theta & \frac{r}{2} \sin \theta \\ \frac{r}{d} & \frac{r}{d} \end{bmatrix} \begin{bmatrix} \omega_r \\ \omega_l \end{bmatrix} \quad (1)$$

From Fig. 1, it is clear that v_r and v_l can be computed from the angular velocities of the mobile robot wheels as $v_r = r\omega_r$ and $v_l = r\omega_l$, respectively. It should also be noted that the kinematics in (1) illustrate the relationship between x, y, θ and ω_r, ω_l that will be utilized later in the development of the discrete optimal controller. The relation in (1) can now be linearized as

$$\dot{Z} = H(z_3)\omega \quad (2)$$

where $\dot{Z} \in \mathbb{R}^3$ is the first time derivative of $Z \in \mathbb{R}^3$, which is defined as $Z \triangleq [z_1 \ z_2 \ z_3]^T$ with $z_1 \triangleq x, z_2 \triangleq y, z_3 \triangleq \theta$, and $H(z_3) \in \mathbb{R}^{3 \times 2}$. When $\omega \triangleq [\omega_r \ \omega_l]^T$ is set to a constant, the expression in (1) can be integrated to obtain the next robot coordinates over a specific period of time as follows, given the initial robot coordinates,

$$\int_{t_0}^t \dot{Z} = \int_{t_0}^t H(z_3)\omega dt \quad (3)$$

and then

$$Z(t) - Z(t_0) = H(z_3)\omega(t - t_0). \quad (4)$$

Further manipulation for the expression in (4) results in

$$Z(t) = Z(t_0) + g(z_3)\omega \quad (5)$$

where $g(z_3) \triangleq H(z_3)\Delta t$ and $\Delta t = (t - t_0)$. From (5), it can be inferred that the desired x, y, θ can be computed from the desired ω according to the definition of Z in (2) and the kinematic model in (5) as follows

$$Z_d(t) = Z_d(t_0) + g(z_{3_d})\omega_d \quad (6)$$

In other words, the desired velocity can be determined from the desired coordinates and orientation of the mobile robot as

$$\omega_d = (g_d^T g_d)^{-1} g_d^T (Z_d(t) - Z_d(t_0)). \quad (7)$$

where $g_d = g(z_{3_d})$. It should be noted that there is a solution ω_d for any desired value of Z_d if $(g_d^T g_d)^{-1}$ is left invertible. However, $(g_d^T g_d)^{-1}$ can be proven to be left invertible as shown in the Appendix I.

B. Dynamics of Two-Wheel Mobile Robot

In order to facilitate the development of the discrete optimal controller, the mobile robot dynamics are essential to be determined. In fact, the dynamics are derived from the mobile robot drive mechanism, which is in this study a differential drive utilizing two dc motors to drive two wheels. Hence, the dynamics of the mobile robot wheels' motors can be described as

$$\begin{bmatrix} \dot{\omega}_r \\ \dot{\omega}_l \end{bmatrix} = \frac{k_m}{J} \begin{bmatrix} I_{ar} \\ I_{al} \end{bmatrix} - \frac{B}{J} \begin{bmatrix} \omega_r \\ \omega_l \end{bmatrix} - \frac{1}{J} \begin{bmatrix} \tau_{Lr} \\ \tau_{Ll} \end{bmatrix} \quad (8)$$

$$\begin{bmatrix} \dot{I}_{ar} \\ \dot{I}_{al} \end{bmatrix} = \frac{1}{L_a} \begin{bmatrix} V_r \\ V_l \end{bmatrix} - \frac{k_b}{L_a} \begin{bmatrix} \omega_r \\ \omega_l \end{bmatrix} - \frac{R_a}{L_a} \begin{bmatrix} I_{ar} \\ I_{al} \end{bmatrix} \quad (9)$$

that are, in turn, affect the entire mobile robot dynamics.

III. DISCRETE OPTIMAL CONTROLLER DESIGN

To facilitate the development of the discrete optimal controller design, the dynamics in (8) and (9) are formulated in a state-space representation such as

$$\dot{X} = AX + BU - D \quad (10)$$

$$Y = CX \quad (11)$$

where $Y(t) \triangleq [\omega_r \ \omega_l]^T \in \mathbb{R}^2$ is the system outputs, $X(t) \triangleq [x_1 \ x_2 \ x_3 \ x_4]^T \in \mathbb{R}^4$ is the state vector, $x_1 \triangleq \omega_r, x_2 \triangleq \omega_l, x_3 \triangleq I_{ar}, x_4 \triangleq I_{al}$, $U(t) \triangleq [V_r \ V_l]^T \in \mathbb{R}^2$ is the control input, and $D(t) \triangleq \begin{bmatrix} \frac{\tau_{Lr}}{J} & \frac{\tau_{Ll}}{J} & 0 & 0 \end{bmatrix}^T \in \mathbb{R}^4$ is the system disturbance. The matrices $A \in \mathbb{R}^{4 \times 4}, B \in \mathbb{R}^{4 \times 2}$, and $C \in \mathbb{R}^{2 \times 4}$ are the state matrix, input matrix, and output matrix, respectively, and written as

$$A = \begin{bmatrix} -\frac{B}{J} & 0 & \frac{k_m}{J} & 0 \\ 0 & -\frac{B}{J} & 0 & \frac{k_m}{J} \\ -\frac{k_b}{L_a} & 0 & -\frac{R_b}{L_a} & 0 \\ 0 & -\frac{k_b}{L_a} & 0 & -\frac{R_b}{L_a} \end{bmatrix}, \quad (12)$$

$$B = \begin{bmatrix} 0 & 0 \\ 0 & 0 \\ \frac{1}{L_a} & 0 \\ 0 & \frac{1}{L_a} \end{bmatrix}, C = \begin{bmatrix} 1 & 0 & 0 & 0 \\ 0 & 1 & 0 & 0 \end{bmatrix}. \quad (13)$$

The continuous-time state-space representation model in (10) to (13), can now be discretized using the zero-order hold method assuming the input is a staircase. Hence, the discrete-time model can be expressed as in [1]

$$X(k+1) = A_d X(k) + B_d U(k) - D(k) \quad (14)$$

$$Y(k) = C_d X(k) \quad (15)$$

where $X(k)$ is the discrete current state, $X(k + 1)$ is the next discrete current state, k is the sampling instant, and A_d, B_d, C_d are the data of the discrete state-space model.

The proposed discrete optimal controller is designed to obtain a zero-tracking error (i.e., x, y, θ goes to x_d, y_d, θ_d as time goes to infinity) with a minimum amount of effort, by the wheels' motors, to drive the mobile robot along the prescribed desired trajectory. Actually, the desired trajectory is tracked by controlling the angular velocities of the wheels' motors, which will affect the mobile robot coordinates accordingly. The discrete optimal controller is, in fact, designed to compensate for disturbances while tracking. However, to achieve the aforementioned control objective (i.e., x, y, θ goes to x_d, y_d, θ_d as time goes to infinity), the mobile robot system should be checked for controllability. In the simulation section, this will be demonstrated.

To facilitate the discrete optimal controller design, the following cost function is utilized

$$V(E_k) = E_k^T Q E_k + U_k^T R U_k + V(E_{k+1}) \quad (16)$$

where the design parameters $Q \in \mathbb{R}^{4 \times 4}$, and $R \in \mathbb{R}^{2 \times 2}$ are positive definite matrices where their values depend on the needed designed performance. If the controller effort needs to be minimized, R should be chosen with a high value, while if it is needed to increase the response speed, the value of Q should be high. $E \triangleq X_d - X \in \mathbb{R}^4$ is the tracking error, X_d is the desired states (i.e., $\omega_{rd}, \omega_{ld}, I_{ard}, I_{ald}$), and $U_k(E_k)$ is the control input. The subscription k and $k + 1$ represent the sampling instances. In order to minimize the aforementioned cost function, $V(E_k)$, the discrete optimal control law, $U_k(E_k)$, can be designed as

$$U^* = \underbrace{-(R + B_d^T P B_d)^{-1} B_d^T P A_d}_{SF} E(k) \quad (17)$$

where SF is the state feedback and $P \in \mathbb{R}^{4 \times 4}$ is the solution of the following Riccati equation from which the state feedback is found

$$P = A_d^T P A_d + Q - A_d^T P B_d (R + B_d^T P B_d)^{-1} B_d^T P A_d. \quad (18)$$

Provided that the discrete system is controllable and the controller in (17) is designed to minimize the cost function in (16), the optimal cost function, $V^*(E_k)$, can be expressed as

$$V^*(E_k) = \min_{U(k)} (E_k^T Q E_k + U_k^T R U_k + V^*(E_{k+1})). \quad (19)$$

Fig. 2 illustrates the steps to implement the discrete optimal controller while Fig. 3 illustrates the proposed closed-loop system.

IV. DISCRETE PID CONTROLLER DESIGN

The Proportional-Integral-Derivative (PID) controller is well-known and a general-purpose controller that has been

used over the past decades due to its efficient performance in many applications and systems [24]. In general, the PID controller can be tuned in different methods as described in [25]. In this section, a discrete PID controller is implemented using the forward Euler method to control the mobile robot by tracking prescribed desired trajectories as follows

$$U = \left(k_p + k_i T_s \Omega + k_d \frac{N}{1 + N T_s \Omega} \right) E \quad (20)$$

where $\Omega \triangleq \frac{1}{(z-1)}$, z is the operator of the discrete function, T_s is the sampling time, N is the filter coefficient, k_p, k_i , and k_d are the controller gains. Fig. 4 illustrates how the discrete PID controller is implemented on the two-wheel mobile robot where (1), (14), and (15) are utilized. Note that the zero-order hold method is used to discretize each block in the system with a sampling time of 10ms in order to perform an adequate comparison with the proposed discrete optimal controller.

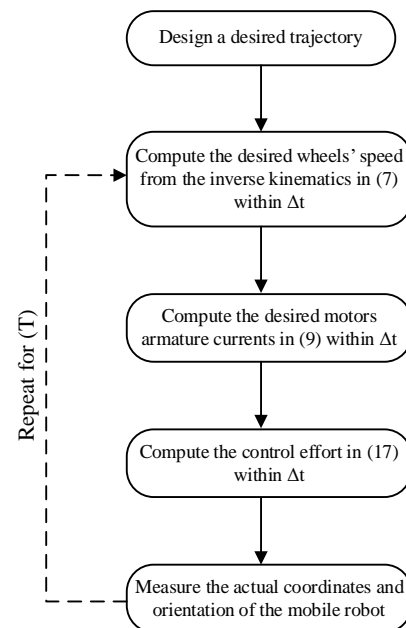


Figure 2. The steps to implement the discrete optimal controller.

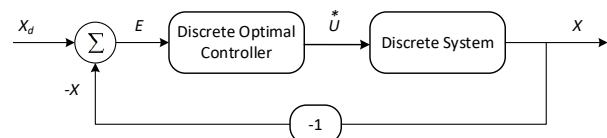


Figure 3. The proposed discrete optimal control system.

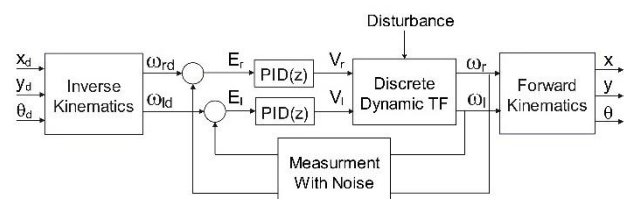


Figure 4. Implementation of the discrete PID on the two-wheel mobile robot.

The desired right and left wheels' angular velocities are calculated as follows

$$\omega_r = \frac{1}{r} \left(V + \frac{d}{2} \omega \right) \quad (21)$$

$$\omega_l = \frac{1}{r} \left(V - \frac{d}{2} \omega \right) \quad (22)$$

V. FUZZY LOGIC CONTROLLER DESIGN

In comparison with the model-based controllers, a Fuzzy Logic Controller (FLC) does not require a priori knowledge of the model to be controlled and that is an advantage of using such a controller [26]. To control the two-wheel mobile robot, fuzzy sets are designed, for each wheel, using two inputs (i.e., mobile robot angular velocity error and its change with respect to time) and one output (i.e., wheel's dc motor input voltage) as follows

$$E \triangleq \omega_d - \omega \quad (23)$$

$$\Delta E \triangleq E_{current} - E_{previous} \quad (24)$$

To elaborate more, Figure 5 illustrates how the FLC controller is implemented on the two-wheel mobile robot where (23) and (24) are utilized.

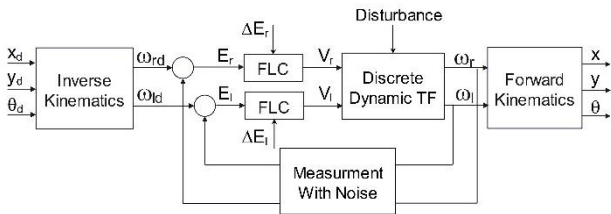


Figure 5. Implementation of the FLC on the two-wheel mobile robot.

Each input-output combination is chosen to have seven membership functions as shown in Table I and Figure 6. The linguistic values for each combination are Negative Big (NB), Negative Medium (NM), Negative Small (NS), Zero (Z), Positive Big (PB), Positive Medium (PM), and Positive Small (PS). According to these values, the Degree of Membership (DOM) is quantified using the (MIN) function.

TABLE I. PROPOSED FUZZY SETS

E \ ΔE	PB	PM	PS	Z	NS	NM	NB
PB	PB	PB	PM	PM	PS	PS	Z
PM	PB	PM	PM	PS	PS	Z	Z
PS	PM	PS	PS	Z	Z	NS	NS
Z	PS	PS	PS	Z	NS	NS	NM
NS	PS	Z	Z	Z	NS	NM	NM
NM	PS	Z	Z	NS	NM	NB	NB
NB	Z	Z	NS	NS	NM	NB	NB

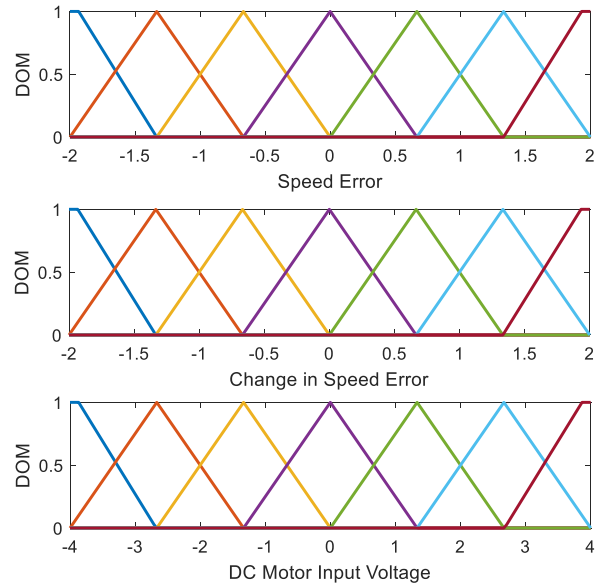


Figure 6. Proposed membership functions for (a) speed error (b) change in speed error, and (c) dc motor input voltage.

After fuzzification, 49 sets are generated to evaluate the output fuzzy set. Based on these sets, a control surface for the proposed FLC can be illustrated as shown in Fig. 7. From the figure, a crisp output value can be defuzzified using the Center of Gravity (COG) method as in [27].

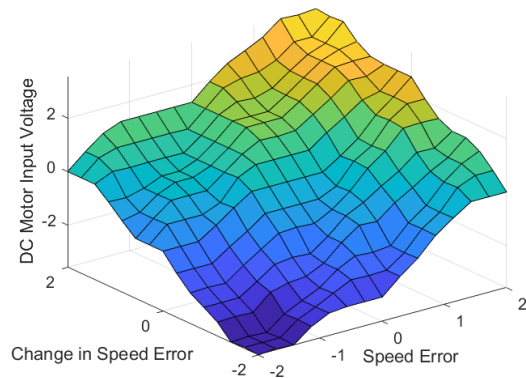


Figure 7. The control surface for the fuzzy controller for both mobile robot wheels.

VI. NUMERICAL SIMULATIONS

In this section, the proposed controller in Section III is implemented and compared with the controllers introduced in Sections IV and V to investigate its tracking performance and effectiveness in controlling a two-wheel mobile robot. For that purpose, error and effort measures are defined as follows

$$EM \triangleq \int_0^T \sqrt{(x_d - x)^2 + (y_d - y)^2 + (\theta_d - \theta)^2} \quad (25)$$

$$REM \triangleq \int_0^T (\tau_r)^2 \quad (26)$$

$$LEM \triangleq \int_0^T (\tau_l)^2$$

where T is the entire simulation time, REM and LEM are the right and left robot wheels' effort measures, respectively, τ_r and τ_l are the right and left robot wheels' generated torques, respectively. It should be noted that to implement the discrete optimal and PID controllers, the dynamic model introduced for the two-wheel mobile robot has to be discretized as in (14) and (15) and then checked for controllability as mentioned earlier. The parameters of the two-wheel mobile robot utilized in the numerical study are listed in Table II. Using the values in Table II, the continuous-time dynamic system model, introduced in (8) and (9), is discretized using the "zero-order hold on the inputs" method in Matlab© with a sampling time of 10ms to obtain the state matrices A_d, B_d and C_d .

TABLE II. PROPOSED TWO-WHEEL MOBILE ROBOT PARAMETERS.

Parameter	Value	Unit
J	0.015	Kg.m ²
B	0.01	N.s/m ²
R_a	0.08	Ω
L_a	36	mH
k_m	0.075	Nm/A
k_b	0.06	V.s/rad
r	9.25	cm
d	37	cm

The developed discrete-time dynamic system model can now be checked for controllability where the controllability matrix is expressed as $G = [B_d \ A_d B_d \ A_d^2 B_d \ A_d^3 B_d]$. Refer to [22] for more details about the values of A_d, B_d and C_d . After substituting A_d, B_d and C_d to compute G , a full rank can be obtained, hence, the system is controllable and then stabilizable. Thus, the discrete optimal controller can be designed.

To investigate the performance and effectiveness of the proposed controllers, two scenarios are introduced to the mobile robot; **Test 1**: no disturbances are applied (i.e., $T_{Lr} = T_{Ll} = 0$), **Test 2**: disturbances are applied on both wheels (e.g., $T_{Lr} = 0.04 \sin(2\pi t)$ and $T_{Ll} = 0.2 \sin(\pi t)$). In both scenarios, the tracked trajectories are (a) circle with a 4m diameter, (b) S-shape (e.g., $X = t - 5$ and $Y = \frac{1}{e^{-3X}}$), and (c) 8-shape (e.g., $X = 1.4 + 0.7 \sin(\frac{\pi t}{15})$ and $Y = 0.6 + 0.7 \sin(\frac{2\pi t}{15})$). In addition, a noise power of 0.0015 is applied to the measurement for all tests to make the simulation more realistic.

A. Discrete Optimal Controller Performance

Under the operating conditions of both Test 1 and Test 2 utilizing the circular trajectory, the tracking performance of the proposed discrete optimal controller can be illustrated in Fig. 8. The right and left angular velocities of the two-wheel mobile robot wheels along with the right and left wheels' motors generated torque are demonstrated in Figs. 9 and 10, respectively. It is clear from Fig. 8 that for Test 1 the mobile robot accurately tracks the trajectory despite of the noisy measurement. It should also be noted

that the red arrows in Fig. 8 indicate the instant orientation of the two-wheel mobile robot while tracking the trajectory.

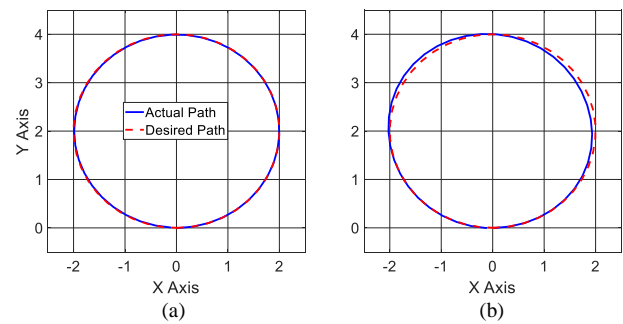


Figure 8. The circular tracking performance of the two-wheel mobile robot using the discrete optimal controller for (a) Test 1 and (b) Test 2, respectively.

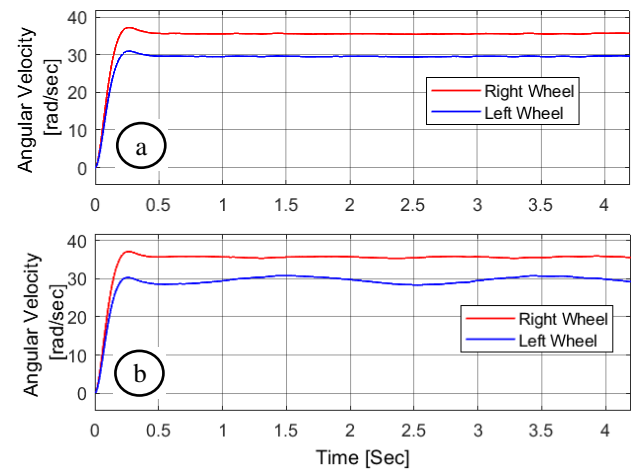


Figure 9. The right and left wheels' angular velocities using the discrete optimal controller for (a) Test 1 and (b) Test 2, respectively, utilizing the circular trajectory.

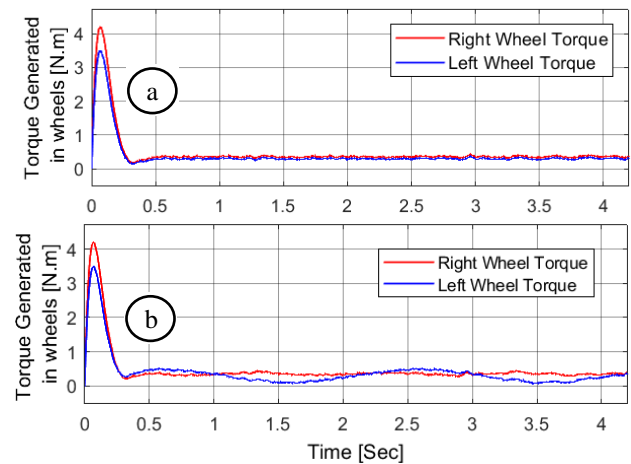


Figure 10. The torques generated in the right and left wheels motors using the discrete optimal controller for (a) Test 1 and (b) Test 2, respectively, utilizing the circular trajectory.

When applying the operating conditions of Test 2, the tracking is more challenging, but the performance is satisfactory despite of the presence of time-varying disturbance torques affecting the robot motion. By comparing the tracking performance of Test 1 with Test 2,

it is clear that the mobile robot exerts relatively more effort (i.e., wheels motors torque) under the operating conditions of Test 2 (refer to Fig. 10). As for the angular velocities, it is observed from Fig. 9 that they are relatively more fluctuating under the operating conditions of Test 2.

Moreover, a desired trajectory of S-shape has been utilized to more challenge the controller. The tracking performance of Test 1 and Test 2 for the discrete optimal controller are shown in Fig. 11. It is clear that the proposed discrete optimal controller demonstrates an adequate performance in Test 1 while it is not so good for Test 2, where there is a noticeable difference between the actual and desired trajectories as illustrated in Fig. 11.

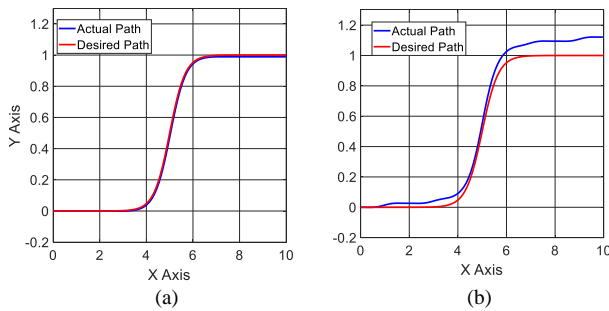


Figure 11. The S-shape tracking performance of the two-wheel mobile robot using the discrete optimal controller for (a) Test 1 and (b) Test 2, respectively.

The right and left angular velocities of the two-wheel mobile robot and the right and left wheels' motors torque are shown in Figs. 12 and 13, respectively. From the figures, it is clear that the angular velocities and generated torques of Test 2 have more fluctuations than those in Test 1 because of the added disturbances. In addition, the generated torques in the wheels' motors needed to overcome these disturbances for Test 2 are relatively more than the ones in Test 1, as shown in the summary table in Section VI.D.

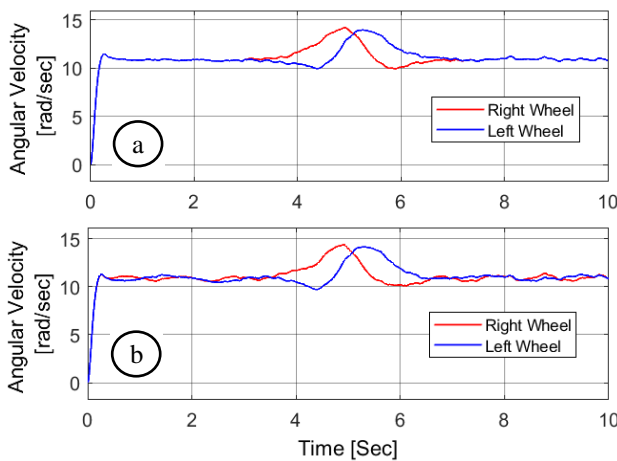


Figure 12. The right and left wheels' angular velocities using the discrete optimal controller for (a) Test 1 and (b) Test 2, respectively, utilizing the S-shape trajectory.

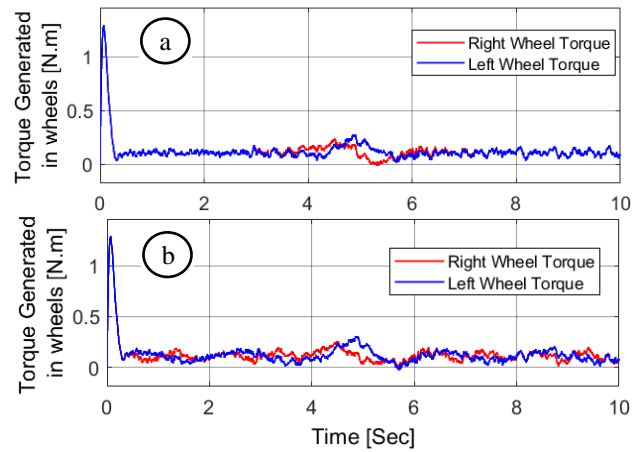


Figure 13. The torques generated in the right and left wheels' motors using the discrete optimal controller for (a) Test 1 and (b) Test 2, respectively, utilizing the S-shape trajectory.

A third trajectory, namely the 8-shape trajectory, is introduced, as well, for the sake of comparison. Test 1 and Test 2 tracking performance is shown in Figure 14. It is clear that the tracking performance is better for Test 1 than Test 2. The right and left angular velocities of the two-wheel mobile robot and the right and left wheels' motors torque for the 8-shape trajectory are illustrated in Figures 15 and 16, respectively. From Figure 15, it is clear that the right and left wheels' angular velocities in Test 2 demonstrate more variations in comparison with the ones in Test 1 due to the added disturbances. The same can be noticed for the torques generated in the right and left wheels' motors in Fig. 16.

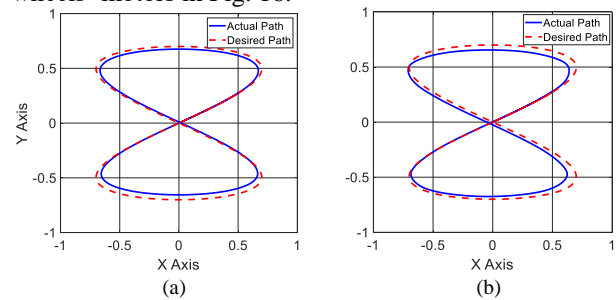


Figure 14. The 8-shape tracking performance of the two-wheel mobile robot using the discrete optimal controller for (a) Test 1 and (b) Test 2, respectively.

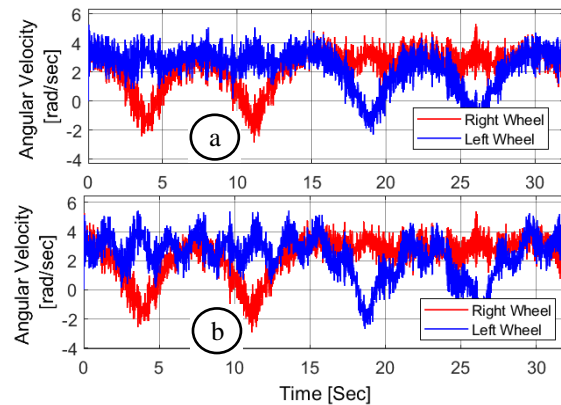


Figure 15. The right and left wheels' angular velocities using the discrete optimal controller for (a) Test 1 and (b) Test 2, respectively, utilizing the 8-shape trajectory.

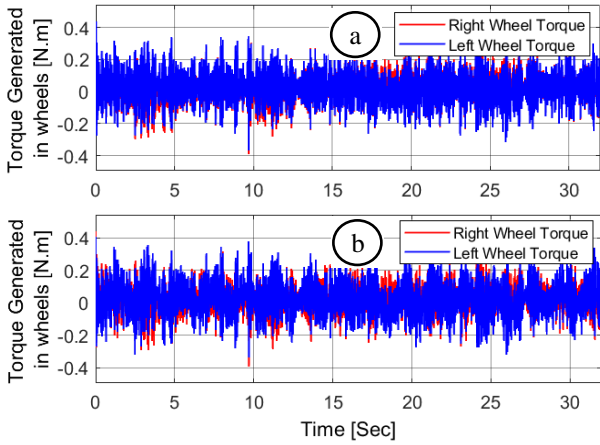


Figure 16. The torques generated in the right and left wheels' motors using the discrete optimal controller for (a) Test 1 and (b) Test 2, respectively, utilizing the 8-shape trajectory.

B. Discrete PID Controller Performance

As mentioned earlier, for the sake of comparison, the performance of a discrete PID controller is investigated under the operating conditions of Test 1 and Test 2. The control gains (e.g., k_p , k_i and k_d) were tuned to be 0.07425, 1.06889, and 0.00125, respectively, in order to provide the best performance possible. The tracking performance of the circular trajectory for Test 1 and Test 2 is illustrated in Figure 17 while the right and left wheels' angular velocities are demonstrated in Figure 18. The right and left wheels' motors torques are presented in Figure 19. It is clear from Figure 17 that the PID controller cannot handle the disturbances in Test 2. There is a significant shift between the desired and actual trajectories. In addition, the wheels' motors generated torque in Test 2 cannot keep the mobile robot on the desired track in comparison with the torques generated by the discrete optimal controller shown in Figure 10.

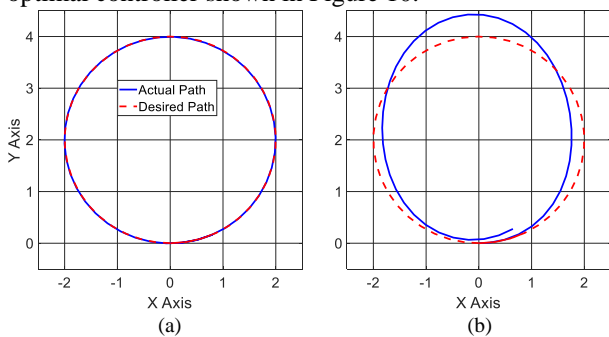


Figure 17. The circular tracking performance of the two-wheel mobile robot using the discrete PID controller for (a) Test 1 and (b) Test 2, respectively.

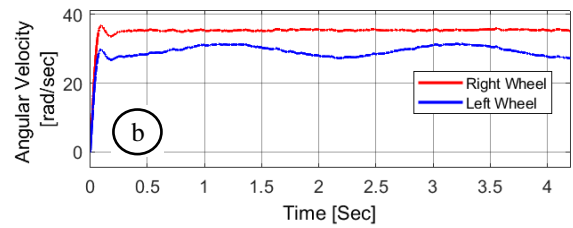
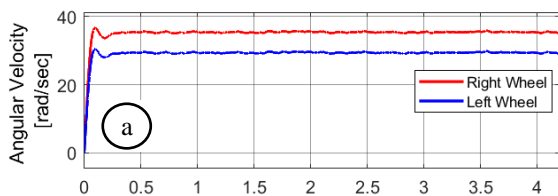


Figure 18. The right and left wheels' angular velocities using the discrete PID controller for (a) Test 1 and (b) Test 2, respectively, for the circular trajectory.

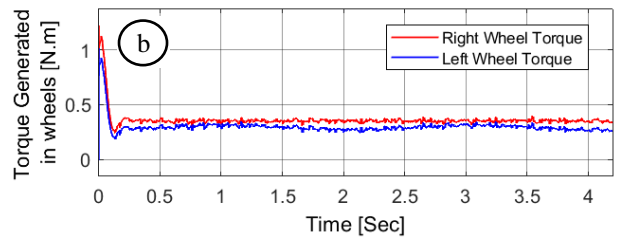
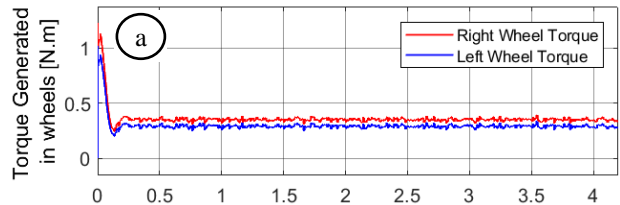


Figure 19. The torques generated in the right and left wheels motors using the discrete PID controller for (a) Test 1 and (b) Test 2, respectively, for the circular trajectory.

The tracking performance, the right and left wheels' angular velocities in addition to the right and left wheels' motors torques for the S-shape and 8-shape trajectories are illustrated in Figs. 20 to 25.

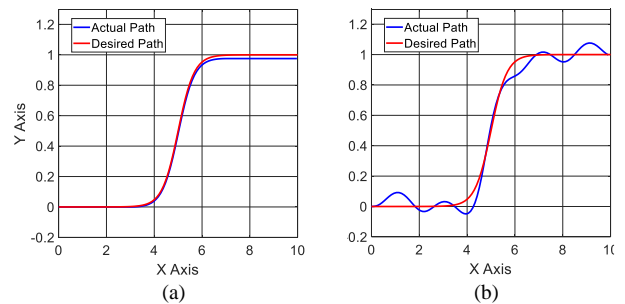
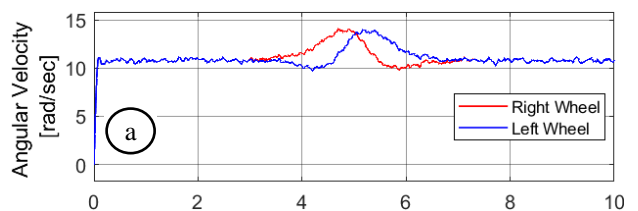


Figure 20. The S-shape tracking performance of the two-wheel mobile robot using the discrete PID controller of (a) Test 1 and (b) Test 2, respectively.



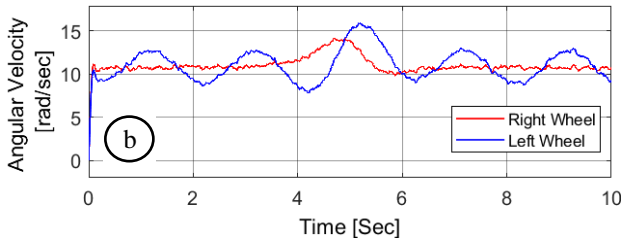


Figure 21. The right and left wheels' angular velocities using the discrete PID controller for (a) Test 1 and (b) Test 2, respectively, utilizing the S-shape trajectory.

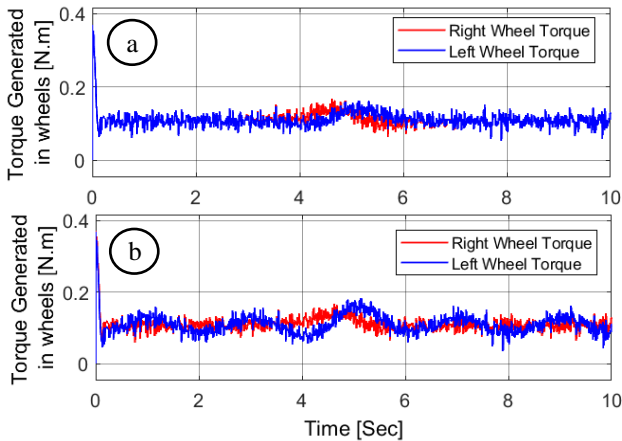


Figure 22. The torques generated in the right and left wheels' motors using the discrete PID controller for (a) Test 1 and (b) Test 2, respectively, utilizing the S-shape trajectory.

Figs. 20 to 22, show that the discrete PID controller cannot handle the S-shape trajectory in Test 2 satisfactorily. From Fig. 20, it is clear that there are ups and downs in the actual trajectory of the mobile robot. It is also obvious from Fig. 22 that the generated torques cannot compensate sufficiently for the added disturbances, which also affect the wheels' angular velocities as shown in Fig. 21. On the other hand, when looking at the 8-shape trajectory, the discrete PID controller exerts more torques, as shown in Fig. 25, to overcome the added disturbances and provides a very satisfactory tracking performance for both Test 1 and Test 2 as shown in Fig. 23. However, that comes with more chattering in the wheels' motors generated torque.

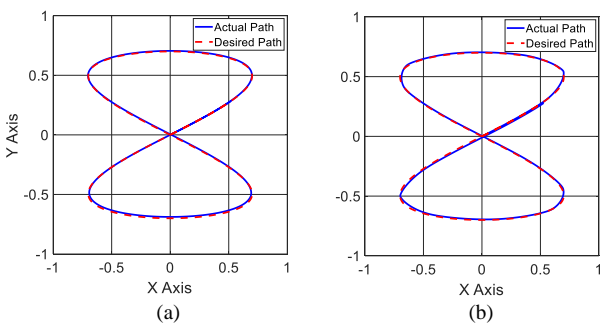


Figure 23. The 8-shape tracking performance of the two-wheel mobile robot using the discrete PID controller for (a) Test 1 and (b) Test 2, respectively.

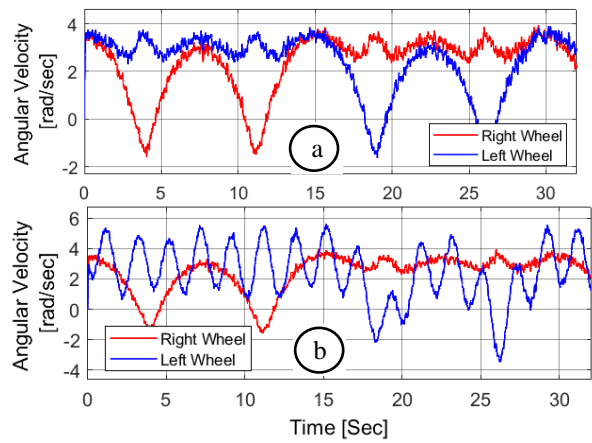


Figure 24. The right and left wheels' angular velocities using the discrete PID controller for (a) Test 1 and (b) Test 2, respectively, utilizing the 8-shape trajectory.

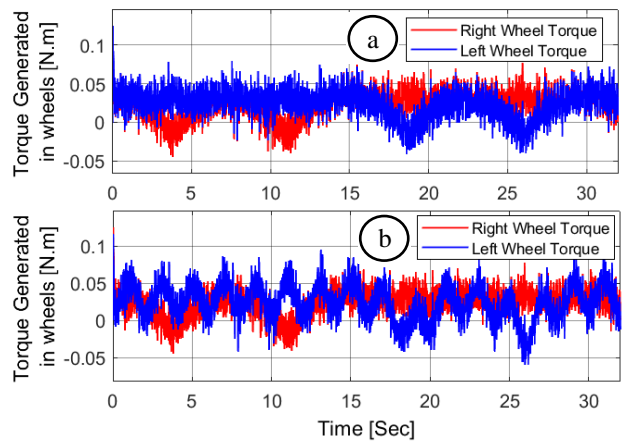


Figure 25. The torques generated in the right and left wheels' motors using the discrete PID controller for (a) Test 1 and (b) Test 2, respectively, utilizing the 8-shape trajectory.

C. Fuzzy Logic Controller Performance

To implement further comparison with the proposed discrete optimal controller, a FLC is investigated under the same operating conditions of Test 1 and Test 2. Utilizing the fuzzy sets, shown in Table I, the membership functions, shown in Fig. 6, and the control surface, shown in Fig. 7, the tracking performance of the circular trajectory in Test 1 and Test 2 is illustrated in Fig. 26. The right and left angular velocities of the two-wheel mobile robot in addition to the right and left wheels' motors torques are demonstrated in Figs. 27 and 28, respectively, for Test 1 and Test 2, respectively.

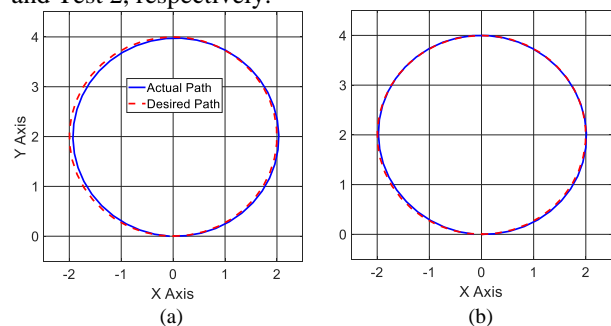


Figure 26. The circular tracking performance of the two-wheel mobile robot using the FLC for (a) Test 1 and (b) Test 2, respectively.

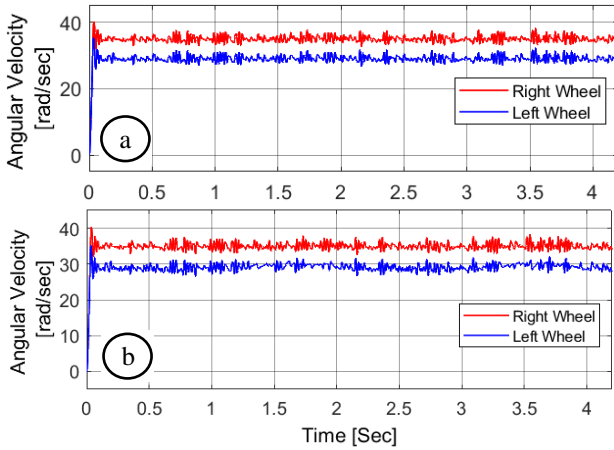


Figure 27. The right and left wheels' angular velocities using the FLC for (a) Test 1 and (b) Test 2, respectively, utilizing the circular trajectory.

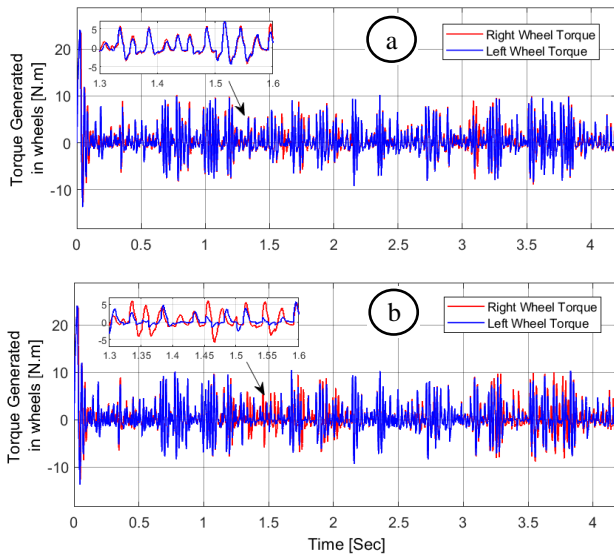


Figure 28. The torques generated in the right and left wheels' motors using the FLC for (a) Test 1 and (b) Test 2, respectively, utilizing the circular trajectory.

The circular tracking performance of the FLC is satisfactory for Test 1 and Test 2. In addition, the FLC circular tracking performance is clearly better than the performance of the discrete PID in Test 2. It is also clear that the FLC generates more fluctuations and chattering in the wheel's angular velocities and wheels' motors torque in comparison with the discrete optimal and PID controllers.

The S-shape and 8-shape trajectories tracking performance are shown in Figs. 29 and 32, respectively. The right and left wheels' angular velocities for the same trajectories are shown in Figs. 30 and 33, respectively, while the generated torques in the right and left wheels' motors are shown in Fig. 31 and 34, respectively. The FLC performs badly, in Test 1, at the last part of the S-shape trajectory while the whole performance in Test 2 is not satisfactory at all as it is clear in Figure 29. Obviously, the angular velocities and generated torques, shown in Figures 30 and 31, are not sufficient to track the desired trajectory for Test 1 and Test 2. However, this inability to track the

S-shape trajectory satisfactorily does not affect the tracking performance of the 8-shape trajectory as shown in Fig. 32. The FLC tracks the 8-shape trajectory with a relatively good performance. However, the angular velocities and the generated torques for both wheels, shown in Figs. 33 and 34, respectively, demonstrate excessive chattering to achieve a satisfactory performance for both tests.

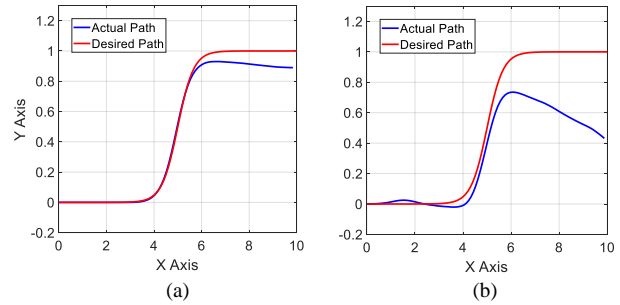


Figure 29. The S-shape tracking performance of the two-wheel mobile robot using the FLC for Test 1 and Test 2, respectively.

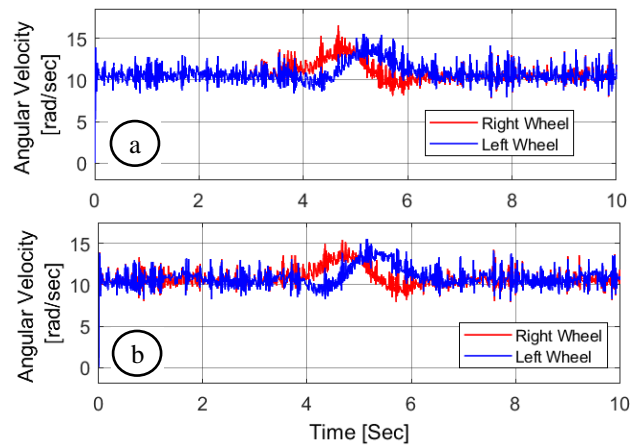


Figure 30. The right and left wheels' angular velocities using the FLC for Test 1 and Test 2, respectively, utilizing the S-shape trajectory.

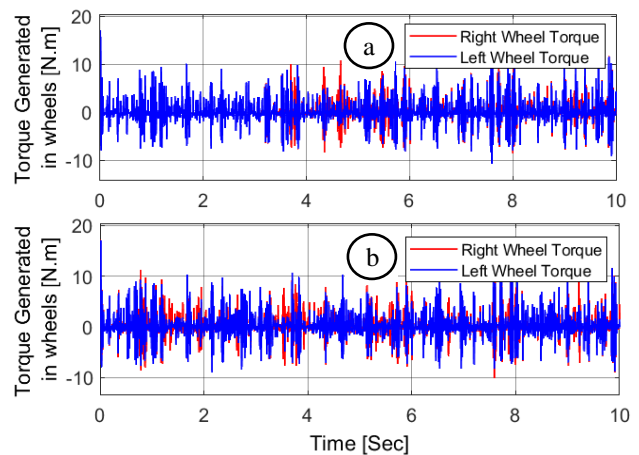


Figure 31. The torques generated in the right and left wheels' motors using the FLC for Test 1 and Test 2, respectively, utilizing the S-shape trajectory.

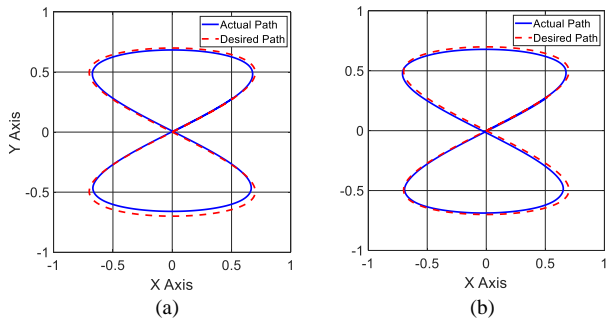


Figure 32. The 8-shape tracking performance of the two-wheel mobile robot using the FLC for Test 1 and Test 2, respectively.

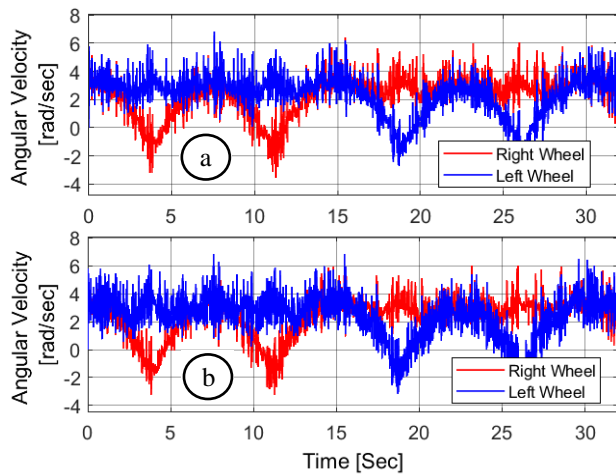


Figure 33. The right and left wheels' angular velocities using the FLC for Test 1 and Test 2, respectively, utilizing the 8-shape trajectory.

D. Controllers Performance Comparison

By observing the results in subsections VI.A, VI.B, and VI.C, it is clear that all proposed controllers perform satisfactorily under the operating conditions of Test 1 utilizing the circular trajectory, where no disturbances are applied. However, when the external disturbances are applied to the mobile robot in Test 2, the FLC controller performs the best and then the discrete optimal, but the discrete PID cannot handle the proposed disturbances. However, this is not true for the S-shape trajectory, where the proposed discrete optimal controller and discrete PID controller did perform satisfactorily for Test 1, but the FLC did not. Furthermore, the performance results in Test 2 were not relatively adequate for all controllers except for the proposed discrete optimal controller up to a certain extent. To more challenge the introduced controllers, an 8-shape trajectory was utilized. The results showed that all the proposed controllers track the desired trajectory satisfactorily. In order to quantify the tracking performance for all introduced controllers, error and effort measures are utilized as defined in (25) and (26). The quantified values are shown in Table III and Table IV. It is clear from these tables that the discrete PID controller is the best controller to track the circular trajectory when no disturbances affect the mobile robot (refer to Test 1) since the EM, REM, and LEM values are the lowest in comparison with the other controllers.

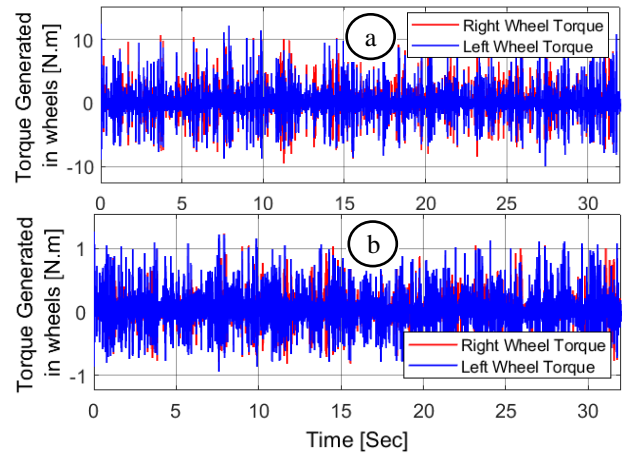


Figure 34. The torques generated in the right and left wheels motors using the FLC for Test 1 and Test 2, respectively, for the 8-shape trajectory.

On the other hand, the EM for the discrete PID controller in all tests utilizing the S-shape and 8-shape trajectories is relatively high. The tables also show that the REM and LEM values for the discrete PID are the lowest in comparison with the discrete optimal controller and FLC and that is expected since the tracking performance is not the best. Note that the discrete PID cannot generate the appropriate amount of torques to force the mobile robot to track different desired trajectories. This makes it not a good choice to control the mobile robot. In this case, the comparison is left to be between the proposed discrete optimal controller and the FLC. According to Tables III and IV, the lowest values of EM, REM, and LEM are for the discrete optimal controller utilizing the S-shape and 8-shape trajectories knowing that the discrete PID controller is out of the comparison. The only case where these values are the lowest using the FLC is for the circular trajectory. As a result, the best tracking performance can be achieved by the proposed discrete optimal controller. The FLC comes next and the discrete PID comes the last.

TABLE III. THE ERROR MEASURE FOR THE THREE PROPOSED CONTROLLERS.

Controller \ Test	Trajectory	Discrete Optimal	Discrete PID	Fuzzy
1	Circle	0.953	0.5134	0.6684
2		0.898	1.375	0.6647
1	S-shape	13.91	13.90	14.01
2		13.79	13.93	14.66
1	8-shape (infinity)	80.63	83.27	82.33
2		80.88	83.31	84.97

TABLE IV. THE REM AND LEM MEASURE FOR THE THREE PROPOSED CONTROLLERS.

Controller	Trajectory	Discrete Optimal		Discrete PID		Fuzzy	
		REM	LEM	REM	LEM	REM	LEM
1	Circle	1.33	0.92	0.58	0.40	1.03	0.83
		2	1.41	1.00	0.66	0.48	1.14
1	S-shape	0.31	0.31	0.13	0.13	0.77	0.74
		2	0.32	0.51	0.14	0.32	0.74
1	8-shape	0.34	0.34	0.03	0.03	1.21	1.16
		2	0.35	0.92	0.05	0.66	1.17

VII. CONCLUSIONS

In this paper, a discrete optimal controller was proposed for two-wheel mobile robots and then compared with a discrete PID and fuzzy controllers. Each of these controllers was tested under the same operating conditions to ensure a fair comparison within two tests utilizing three different trajectories. The first test assumes no disturbances and the other test assumes disturbances are applied on both wheels of the mobile robot. Moreover, error and effort measures were utilized to compare the tracking performance quantifiably for the introduced controllers. From testing the controllers in a numerical environment, they showed a satisfactory tracking performance when no disturbances were applied. On the other side, the discrete optimal controller showed the best performance when disturbances are applied on the mobile robot wheels while the discrete PID and fuzzy controllers were unable to compensate for these disturbances and could not track some desired trajectories.

APPENDIX I: PROOF THAT $(g_d^T g_d)^{-1}$ IS LEFT INVERTIBLE

If $(g_d^T g_d)^{-1}$ is left invertible, then the determinant of $(g_d^T g_d) \neq 0$. To elaborate more

$$g_d^T g_d = \begin{bmatrix} \frac{r}{2} \cos \theta_d & \frac{r}{2} \sin \theta_d & \frac{r}{d} \\ \frac{r}{2} \cos \theta_d & \frac{r}{2} \sin \theta_d & -\frac{r}{d} \end{bmatrix} \begin{bmatrix} \frac{r}{2} \cos \theta_d & \frac{r}{2} \cos \theta_d \\ \frac{r}{2} \sin \theta_d & \frac{r}{2} \sin \theta_d \\ \frac{r}{d} & -\frac{r}{d} \end{bmatrix} = \begin{bmatrix} \frac{r^2}{4} + \frac{r^2}{d^2} & \frac{r^2}{4} - \frac{r^2}{d^2} \\ \frac{r^2}{4} - \frac{r^2}{d^2} & \frac{r^2}{4} + \frac{r^2}{d^2} \end{bmatrix} \quad (I.1)$$

where the determinant of the expression in (I.1) is

$$\Delta g_d^T g_d = \left(\frac{r^2}{4} + \frac{r^2}{d^2}\right)^2 - \left(\frac{r^2}{4} - \frac{r^2}{d^2}\right)^2 \quad (I.2)$$

And since $\left(\frac{r^2}{4} + \frac{r^2}{d^2}\right) \neq \left(\frac{r^2}{4} - \frac{r^2}{d^2}\right)$, hence, $\Delta g_d^T g_d \neq 0$.

CONFLICT OF INTEREST

The authors declare no conflict of interest.

AUTHOR CONTRIBUTIONS

Conceptualization, A. Al-Tamimi, and Ah. Al-Jarrah; methodology, A. Al-Tamimi, and F. Al-Momani; software, F. Al-Momani, and M. Salah; validation, F. Al-Momani; formal analysis, A. Al-Tamimi, and M. Salah; investigation, F. Al-Momani; resources, Ay. Al-Jarrah; data accurate, F. Al-Momani, and Ah. Al-Jarrah; writing—original draft preparation, F. Al-Momani, and Ay. Al-Jarrah; writing—review and editing, M. Salah, and Ah. Al-Jarrah; visualization, F. Al-Momani, and Ah. Al-Jarrah; supervision, A. Al-Tamimi, and M. Salah; project administration, F. Al-Momani, and M. Salah.

REFERENCES

- [1] R. Francisco, F. Valero, and C. Llopis-Albert, "A review of mobile robots: Concepts, methods, theoretical framework, and applications," *International Journal of Advanced Robotic Systems*, vol. 16, no. 2, 2019.
- [2] N. Leena and K. K. Saju, "Modelling and trajectory tracking of wheeled mobile robots," *Procedia Technology*, vol. 24, pp. 538-545, 2016.
- [3] J. Abhishek and M. Kumar, "Two wheels differential type odometry for mobile robots," in *Proc. of 3rd International Conference on Reliability, Infocom Technologies and Optimization*, IEEE, 2014.
- [4] H. M. Zhang and M. L. Li, "Rapid path planning algorithm for mobile robot in dynamic environment," *Advances in Mechanical Engineering*, vol. 9, no. 12, 2017.
- [5] T. Sebastian, W. Burgard, and D. Fox, "A real-time algorithm for mobile robot mapping with applications to multi-robot and 3D mapping," in *Proc. 2000 ICRA. Millennium Conference. IEEE International Conference on Robotics and Automation. Symposia Proceedings (Cat. No. 00CH37065)*, vol. 1, IEEE, 2000.
- [6] Pfister, T. Samuel, S. I. Roumeliotis, and J. W. Burdick, "Weighted line fitting algorithms for mobile robot map building and efficient data representation," in *Proc. 2003 IEEE International Conference on Robotics and Automation (Cat. No. 03CH37422)*, vol. 1, IEEE, 2003.
- [7] Briskin, S. Eugene, et al, "Mathematical modelling of mobile robot motion with propulsio device of discrete interacting with the support surface," *IFAC-PapersOnLine*, vol. 51, no. 2, pp. 236-241, 2018.
- [8] A. Lazarowska, "Discrete artificial potential field approach to mobile robot path planning," *IFAC-PapersOnLine*, vol. 52, no. 8, pp. 277-282, 2019.
- [9] Schmidt, K. Werner, and Y. S. Boutalis, "Fuzzy discrete event systems for multiobjective control: Framework and application to mobile robot navigation," *IEEE Transactions on Fuzzy Systems* vol. 20, no. 5, pp. 910-922, 2012.
- [10] Farooq, Umar, et al. "Fuzzy logic based path tracking controller for wheeled mobile robots," *International Journal of Computer and Electrical Engineering*, vol. 6, no. 2, p. 77, 2014.
- [11] Al-Dahhan, M. R. Hashim, and M. M. Ali, "Path tracking control of a mobile robot using fuzzy logic," in *Proc. 2016 13th International Multi-Conference on Systems, Signals & Devices (SSD)*, IEEE, 2016.
- [12] N. Mohamed, et al, "Mobile robot visual navigation based on fuzzy logic and optical flow approaches," *International Journal of System Assurance Engineering and Management*, vol. 10, no. 6, pp. 1654-1667, 2019.
- [13] D. Faik and M. Kalyoncu, "Differential drive mobile robot trajectory tracking with using pid and kinematic based backstepping controller," *Selçuk Üniversitesi Mühendislik, Bilim ve Teknoloji Dergisi*, vol. 5, no. 1, pp. 1-15, 2017.
- [14] X. Qing, et al. "Fuzzy PID based trajectory tracking control of mobile robot and its simulation in Simulink," *International Journal of Control and Automation*, vol. 7, no. 8, pp. 233-244, 2014.

- [15] Y. M. Liang, et al. "Adaptive fuzzy control for trajectory tracking of mobile robot," in *Proc. 2010 IEEE/RSJ International Conference on Intelligent Robots and Systems*, IEEE, 2010.
- [16] H. W. Mo, Q. R. Tang, and L. L. Meng, "Behavior-based fuzzy control for mobile robot navigation," *Mathematical Problems in Engineering*, 2013.
- [17] M. Thi, Thoa, et al. "MIMO fuzzy control for autonomous mobile robot," *Journal of Automation and Control Engineering*, vol. 4, no. 1, pp. 65-70, 2016.
- [18] B. Moudoud, H. Aissaoui, and M. Diany, "Robust adaptive trajectory tracking control based on sliding mode of electrical wheeled mobile robot," *International Journal of Mechanical Engineering and Robotics Research*, vol. 10, no. 9, pp. 505-509, 2021.
- [19] A. Amin, et al. "Feasibility assessment of Kian-I mobile robot for autonomous navigation," *Neural Computing and Applications*, vol. 34, no. 2, pp. 1199-1218, 2022.
- [20] Moshayedi, A. Jahangir, J. S. Li, and L. F. Liao, "Simulation study and PID Tune of Automated Guided Vehicles (AGV)," in *Proc. 2021 IEEE International Conference on Computational Intelligence and Virtual Environments for Measurement Systems and Applications (CIVEMSA)*. IEEE, 2021.
- [21] Moshayedi, A. Jahangir, et al. "Path planning and trajectory tracking of a mobile robot using bio-inspired optimization algorithms and PID control," in *Proc. 2019 IEEE International Conference on Computational Intelligence and Virtual Environments for Measurement Systems and Applications (CIVEMSA)*. IEEE, 2019.
- [22] F. Al-Momani, A. Al-Tamimi, A. Al-Jarrah, and M. Salah, (2021, November). "Discrete optimal tracking control for a two-wheel mobile robot driven by DC motors," Presented at 2021 IEEE Jordan International Joint Conference on Electrical Engineering and Information Technology (JEEIT) Amman, Jordan, November (pp. 25-30). 2021.
- [23] A. J. Moshayedi, et al. "Review on: The service robot mathematical model," *EAI Endorsed Transactions on AI and Robotics*, vol. 1, pp. 1-19, 2022.
- [24] B. Alexandru, "Position control of a mobile robot through PID controller," *Acta Universitatis Cibiniensis. Technical Series*, vol. 71, no. 1, pp. 14-20, 2019.
- [25] A. J. Moshayedi, A. S. Roy, and L. F. Liao, "PID tuning method on AGV (Automated Guided Vehicle) industrial robot," *Journal of Simulation and Analysis of Novel Technologies in Mechanical Engineering*, vol. 12, no. 4, pp. 53-66, 2019.
- [26] B. Siddhartha and P. Dutta, "Fuzzy logic: Concepts, system design, and applications to industrial informatics," *Handbook of Research on Industrial Informatics and Manufacturing Intelligence: Innovations and Solutions*, IGI Global, 2012, pp. 33-71.
- [27] T. A. Runkler, "Selection of appropriate defuzzification methods using application specific properties," *IEEE Transactions on Fuzzy Systems*, vol. 5, no. 1, pp. 72-79, 1997.

Copyright © 2022 by the authors. This is an open access article distributed under the Creative Commons Attribution License (CC BY-NC-ND 4.0), which permits use, distribution and reproduction in any medium, provided that the article is properly cited, the use is non-commercial and no modifications or adaptations are made.



Fadwa Al-Momani is an assistant tutor in the Department of Mechatronics Engineering at the Hashemite University. She received her M.S. and B.Sc. degrees in Mechatronics Engineering from Al-Balqa' Applied University in 2012 and 2007, respectively. Her research interests include control systems, modeling, electrical machines, and transducers.
E-mail: fadwamomani@hu.edu.jo.



Asma Al-Tamimi is an associate professor in the Department of Mechatronics Engineering at the Hashemite University. She received her Ph.D. and M.S in Electrical Engineering from the University of Texas at Arlington, Texas, USA, in July 2007 and 2003, respectively, and her B.Sc. in Electromechanical Engineering from Al-Balqa' Applied University in June 1999. She is the author of one book, two book chapters, and many refereed journal and international conference articles.
E-mail: altamimi@hu.edu.jo



Ahmad Al-Jarrah is an associate professor in the Department of Mechatronics Engineering at the Hashemite University. He received his Ph.D. in Mechanical Engineering from the University of Ottawa, Ontario, Canada, in January 2007. He also worked as an assistant professor in the Department of Mechanical Engineering at Umm Al Qura University, KSA. In May 2016, he became an associate professor which qualified him to get the opportunity of spending his sabbatical leave as a visiting professor at the School of Electrical Engineering and Computer Science (EECS), University of Ottawa. Dr. Al-Jarrah was involved in many collaborative research projects financed by The Hashemite University and other instances in mechatronics systems and applications. His research of interest includes intelligent systems, linear and nonlinear control systems, automotive systems, control of MEMS, and robotics applications.
E-mail: jarrah@hu.edu.jo



Ayat Al-Jarrah received the M.S. in Mechanical Engineering from Jordan University of Science and Technology in 2011. She currently works as an instructor in the department of Mechatronics Engineering at the Hashemite University. Her research interests include control systems, modeling, and energy systems.
E-mail: ayataljarrah@hu.edu.jo



Mohammad Salah is a professor in the Department of Mechatronics Engineering at the Hashemite University. He received his Ph.D. in Electrical Engineering from Clemson University, South Carolina, USA, in July 2007, his M.S. in Electrical Engineering from the University of New Hampshire, New Hampshire, USA, in December 2003, and his B.Sc. in Technological Engineering from Al-Balqa' Applied University in June 2000. He also worked for PALCO Control as a mechatronics and control engineer from June 2000 to January 2002. He authored two books and many international refereed journal and conference articles. His research interests include applications of nonlinear control design in mechatronics systems, automotive and hybrid systems, robotics systems, and renewable energy systems.
E-mail: msalah@hu.edu.jo